Applied Catalysis B: Environmental 182 (2016) 142–152

Contents lists available at ScienceDirect

Applied Catalysis B: Environmental

journal homepage: www.elsevier.com/locate/apcatb

Sol–gel synthesised WO_3 nanoparticles supported on mesoporous silica for liquid phase nitration of aromatics

A.B. Kulal[a,b], M.K. Dongare[a,c], S.B. Umbarkar[a,b,*]

[a] Catalysis Division, CSIR-National Chemical Laboratory, Pune 411008, India
[b] Academy of Scientific and Innovative Research, CSIR, Anusandhan Bhawan, New Delhi 110 001, India
[c] Malati Fine Chemicals Pvt. Ltd., 4/A Durvankurdarshan Society, Panchawati, Pune 411008, India

ARTICLE INFO

Article history:
Received 3 July 2015
Received in revised form 18 August 2015
Accepted 10 September 2015
Available online 11 September 2015

Keywords:
Heterogeneous catalysis
Aromatic nitration
Regioselective
Sol–gel synthesis
Water polarization

ABSTRACT

A series of WO_3/SiO_2 catalysts have been prepared by sol-gel method using ammonium metatungstate and ethyl silicate-40 (ES-40) as WO_3 and SiO_2 precursors respectively. The sol-gel method has led to the formation of WO_3 nano-particles of 2–5 nm well dispersed on mesoporous silica along with some WO_3 agglomerates. Formation of monoclinic WO_3 was seen on the catalysts above 5 wt% WO_3 loading by XRD analysis. Silica has shown very high surface area of 606 m^2/g which decreased gradually upto 368 m^2/g with 20 wt% WO_3 loading. 20 wt% WO_3/SiO_2 catalyst has shown maximum acidity (0.56 mmol NH_3/g) with presence of both Lewis and Brønsted acidity. UV–vis DRS analysis showed formation of polytungstate species along with WO_3 on silica surface. The prepared catalysts were used for liquid phase nitration of aromatics using 70% nitric acid as nitrating agent without using any sulfuric acid. Very high conversion (99%) was obtained for *p*-cresol nitration with very high selectivity (99%) for 2-nitro *p*-cresol. The water formed during the reaction was removed azeotropically using ethylene dichloride as solvent. In case of *o*-xylene 74% conversion was obtained with 54% selectivity for 4-nitro *o*-xylene. The effect of different WO_3 precursors on nitration efficiency was studied using sodium tungstate and tungstic acid as precursors. However,ammonium metatungstate showed the highest acidity. Sodium tungstate showed formation of dimer of sodium tungstate which did not show any acidity and hence no activity for nitration. The mechanism for nitration using WO_3/SiO_2 has been proposed based on polarisation of water on tungsten centre generating Brønsted acidity which can further generate nitronium ion giving subsequently nitration of the aromatic ring.

1. Introduction

Nitration of aromatics is an important chemical transformation that offers an efficient, atom economical route to nitrogen-containing molecules in organics [1]. These nitro aromatics are important building blocks in synthetic organic chemistry. Explosives and precursors for azo dyes are the major applications of nitro aromatics apart from pharmaceuticals, materials and precursors for other diverse functional groups. There are many book chapters and review articles published on nitrations by Ingold [2], Olah [3,4], Schofield [5,6], Ione [7] and Goubing Yan [8]. Traditionally nitration is carried out by using mixture of concentrated nitric acid (98%) and sulphuric acid in the proportion of 1:2. Even though nitrating mixture has very high efficiency in terms of conversion, it has some drawbacks such as the low regioselectivity and poor tolerance for functional groups apart from generation of large quantity of dilute sulphuric acid which leads to environmental hazards [9–11]. Sulphuric acid acts as catalyst for generation of nitronium ion by protonation of the nitric acid. Sulphuric acid also acts as dehydrating agent and heat sink for the highly exothermic reaction [12]. Due to the formation of water as one of the product, large quantity of dilute sulphuric acid is generated. As dilute sulphuric acid cannot be used for nitration, it has to be concentrated for recycling, which is an energy intensive and costly process. The disposal of such large quantity of dilute sulphuric acid poses environmental problems, making nitration of aromatic compounds one of the most hazardous industrial processes.

Nitration using solid acid catalyst without sulfuric acid would be an attractive alternative. Various types of solid acids have been explored for this transformation. Solid acid effectively plays role of sulfuric acid to form nitronium ion hence solid acid with Brønsted

* Corresponding author at: Catalysis Division, CSIR-National Chemical Laboratory, Pune, 411008, India. Fax: +91 2025902633.
E-mail address: sb.umbarkar@ncl.res.in (S.B. Umbarkar).

http://dx.doi.org/10.1016/j.apcatb.2015.09.020
0926-3373/

acidity is essential [13]. Processes are being developed to reduce the spent acid generated during this reaction and to get the maximum conversion with selectivity for desired product. Solid acid catalysts so far used are zeolites [14], H-beta zeolite [15], clay supported metal nitrates [16], Fe^{3+} on K-10 montmorillonite [17], sulphated titania [18], sulphated SnO_2 [19], modified silica [7,20], silica supported Cs modified heteropolyacid [21], MCM-41 [22], MoO_3/SiO_2 [13], heteropolyacids [23] etc.

Various solid acid catalysts have been used for vapor phase and liquid phase nitrations using range of nitrating agents. *o*-xylene nitration has been carried out before using zeolites like H-β, H-ZSM-5 as well as MoO_3/SiO_2 and 70% HNO_3 as nitrating agent [24]. Maximum 70% *o*-xylene conversion has been reported with H-β though with only 26% selectivity for 4-NOX. It was shown that at lower conversion the selectivity for 4-NOX was higher but with increase in the conversion, selectivity for NOX decreased significantly with corresponding increase in oxidation products and side chain nitration products. MoO_3/SiO_2 catalyst has been used extensively in the literature including our group for various acid catalysed reactions including vapour and liquid phase nitrations. Mixed oxides WO_3–MoO_3 prepared by wet grinding has been reported by Sato and Hirose [25] for vapour phase nitration of benzene using NO_2 (2.3 equivalent) to yield ~25% nitrobenzene at 200 °C. MoO_3/SiO_2 has shown very high efficiency for vapour phase nitration of benzene [26]. However when the same catalyst was used for liquid phase nitration of cumene, all the possible products like o, m and *p*-nitrocumenes as well as oxidation and side chain nitrated products were obtained with almost equal selectivity at maximum conversion (~60%) [13]. The same catalyst when used for phenol nitration at RT using 50 wt% catalyst loading gave only 48% conversion with maximum selectivity for 2-nitrophenol [15]. There are several sulfated solid acid catalysts reported for liquid phase nitration of aromatics. Sulfated carbon along with $NaNO_3$ as nitrating agent with as high as 70 wt% catalyst loading has been reported for solvent free nitration of range of aromatics at room temperature [27]. Sulphated MCM-41 with 2–8% H_2SO_4 loading has been used for nitration of phenol with 25 wt% catalyst loading and 30% HNO_3 as nitrating agent with very high conversion upto 93% though with predominant (90%) selectivity for *o*-nitrophenol [22]. Nanoscopic sulfated titania and iron doped sulfated titania has been used for nitration of phenol at 0 °C to give ~86% conversion and >90% selectivity for *o*-nitrophenol. In this case some amount of trinitrophenol (1–4% selectivity) is also formed which is explosive in nature [18]. Tungsten oxide supported on sulphated tin oxide has also been used for nitration of phenol with upto 98% conversion with maximum selectivity for *o*-nitrophenol [19]. Phenol nitration has also been reported using immobilised heteropoly acid like silicotungstic acid on zirconia (15% loading) with very high conversion upto 95% with *o*-nitrophenol as a major product (91% selectivity) [23]. Choudary et al. [17] have used Fe-montmorillonite clay for liquid phase chlorobenzene nitration with very high conversion upto 90%, however the nitrating agent used was mixture of acetic anhydride and fuming nitric acid. Phosphoric acid supported on montmorillonite clay has been studied for nitration of bromobenzene using 1.5 equivalent HNO_3. Though the yields of nitrobromobenzene were in the range of 35–97% the leaching of phosphioric acid was observed and it was necessary to regenerate the catalyst by treating with H_2PO_4.

In recent years, many efforts have been devoted to develop a nitration procedure by using different nitrating agents like NO_2 (N_2O_5) [28], nitrate salts [27], alkyl and acyl nitrates [25] as well as nitronium tetrafluoroborate [29]. Very high efficiency has been reported with some metal nitrates as nitrating agents. Bismuth nitrate with montmorillonite clay as catalyst has given almost 99% yield in only 10 min [30]. Mixture of calcium nitrate and acetic acid has also been used for microwave assisted nitrations. Efficient and regioselective phenol nitration was reported using nickel nitrate as nitrating agent with *p*TSA as catalyst [31]. Additionally, selective mononitration of phenols was achieved using ionic liquids [32]. Ipso nitration of aryl boronic acid has been carried out using metal nitrates and trimethylsilyl chloride [33]. Though high yield and regioselectivity are some of the advantages of metal nitrates as nitrating agent; generation of stoichiometric quantities of metal salts as byproduct is the major disadvantage making it non atom economic as well as environmentally hazardous. Although each method has some advantages over other, some of them need drastic reaction conditions such as high pressure, high temperature etc., as well as critical handling processes for unstable nitrating agents [16,28,12]. Considering all these facts the best suited nitration process for industry would be liquid phase nitration using commercial 70% nitric acid as nitrating agent. Thus there is still scope to develop a stable and eco-friendly alternative to sulphuric acid.

In the present work we have prepared a series of WO_3/SiO_2 solid acid catalysts by simple sol–gel method with varying amount of WO_3 and WO_3 precursors and used for liquid phase nitration of aromatics and the results are presented herein.

2. Experimental

2.1. Materials

All the reagents viz., ammonium metatungstate (AMT), tungstic acid (TA), sodium tungstate (NaT), ethyl silicate-40 (ES-40) (Chemplast, Chennai, CAS registry no. 18,945-71-7), *iso*-propyl alcohol (IPA), 50% aq. hydrogen peroxide, 25% aq. ammonium hydroxide solution, *o*-xylene, 70% aq. HNO_3, ethylene dichloride were procured from Thomas Baker, LOBA and Merck chemicals, India and used as such without further purification.

2.2. Catalyst preparation

The WO_3/SiO_2 (WS) catalysts with varying WO_3 loading ranging from 1 to 30 wt% were synthesized by sol–gel technique using ES-40 as silica precursor and three different WO_3 precursors viz., ammonium metatungstate (AMT), tungstic acid (TA) and sodium tungstate (NaT). The typical synthesis procedures for 20WS are described below.

2.2.1. Sol–gel synthesis of 20WS catalyst using AMT as WO_3 precursor

In a typical procedure, 20WS catalyst was synthesized by dissolving 5.31 g AMT in 10 mL distilled water. This solution was added drop wise to the dry IPA solution (35 mL) of ES-40 (50.0 g) with constant stirring. To this solution 3 mL dil. NH_4OH (2.5%) solution was added. The solution was stirred until white gel was obtained. The resultant gel was air dried and further calcined at 500 °C in air in a muffle furnace for 5 h. Similarly catalysts with 1, 5, 10, 15, 25 and 30 wt% tungsten oxide loadings were prepared and named *x*WSAMT where *x* corresponds to the wt% loading of WO_3, e.g. 20WSAMT corresponds to 20 wt% WO_3 loading on silica using AMT as precursor.

2.2.2. Sol–gel synthesis of 20WS catalyst using TA as WO_3 precursor

In a typical procedure, 5.39 g tungstic acid was separately dissolved in 50 mL 50% aqueous hydrogen peroxide, 5 mL water and 7 mL 25% dil. NH_4OH. This solution was added drop wise to the dry IPA (35 mL) solution of ES-40 (50.0 g) with constant stirring. The solution was kept overnight until an opaque gel was obtained. This resultant gel was air dried and further calcined at 500 °C in air in a muffle furnace for 5 h and the catalyst was named as 20WSTA.

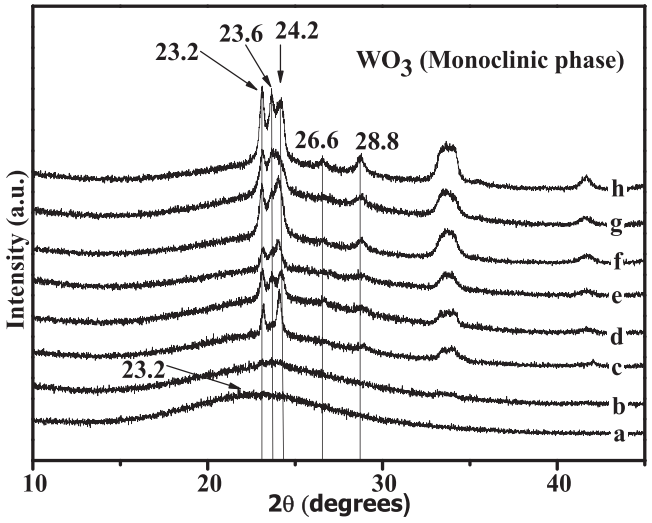

Fig. 1. XRD patterns of (a) SiO_2, (b) 1WSAMT, (c) 5WSAMT, (d) 10WSAMT, (e) 15WSAMT, (f) 20WSAMT, (g) 25WSAMT and (h) 30WSAMT.

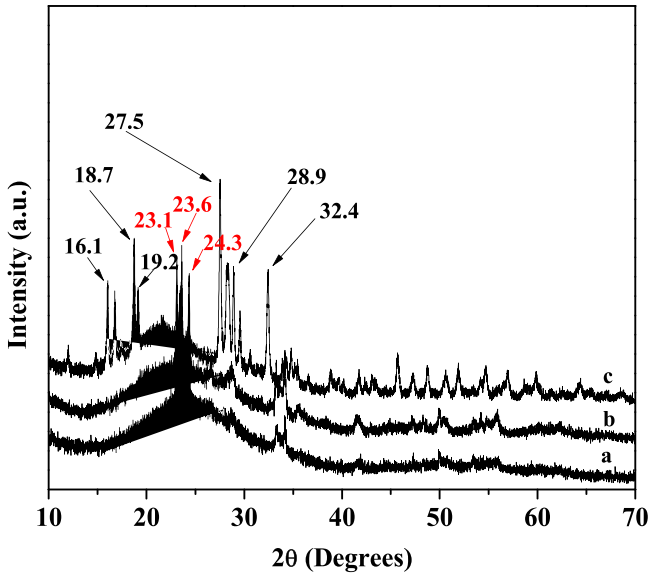

Fig. 2. The XRD patterns of (a) 20WSAMT, (b) 20WSTA and (c) 20WSNaT.

2.2.3. Sol–gel synthesis of 20WS catalyst using NaT as WO_3 precursor

In a typical procedure, 7.11 g NaT was separately dissolved in 20 mL water. This solution was added drop wise to the dry IPA (35 mL) solution of ES-40 (50.0 g) with constant stirring. After obtaining clear solution 3 mL dil. NH_4OH (2.5%) solution was added and stirred till white gel was formed. The resultant gel was air dried and further calcined at 500 °C in air in a muffle furnace for 5 h and the catalyst was named as 20WSNaT.

2.3. Catalyst characterization

2.3.1. Powder X-ray diffraction analysis

X-ray diffraction patterns of prepared catalysts were recorded on PAN analytical X'Pert Pro Dual Goniometer diffractometer. X'celerator solid state detector was employed for the experiments with CuKα (1.542 Å) radiation and a Ni filter.

2.3.2. BET surface area analysis

The BET surface area of the calcined samples was determined by N_2 sorption at −196 °C using NOVA 1200 (Quanta Chrome) equipment. Prior to N_2 adsorption, the materials were evacuated at 300 °C under vacuum. The specific surface area, BET, was determined according to the BET equation.

2.3.3. Fourier transformed infrared spectroscopic studies

The Fourier transform infrared (FT-IR) spectra of the samples were recorded on a Thermo Nicolet Nexus 670 IR instrument under ambient conditions using KBr pellets with a resolution of 4 cm^{-1} in the range of 4000–400 cm^{-1} averaged over 100 scans.

2.3.4. Raman spectroscopic studies

Raman spectra of the catalysts were recorded on a HR 800 LabRAM infinity spectrometer (Horiba-Jobin-Yvon) equipped with a liquid nitrogen cooled detector and a He–Ne laser supplying the excitation line at 632 nm with 1–10 mW power and a resolution of 0.35 cm^{-1}.

2.3.5. UV–vis DRS studies

The UV–vis DRS spectra of the catalyst samples were recorded on a PerkinElmer Lambda 650 UV–vis DRS spectrometer equipped with an integration sphere diffused reflectance attachment. The spectra were obtained in the range of 200–800 nm against the $BaSO_4$ as reference.

2.3.6. Acidity measurements

The NH_3-TPD experiments were performed using a Micromeritics Autochem 2910 instrument. A weighed amount of the sample (~100 mg) was placed in a quartz reactor, pretreated in a flow of He gas at 500 °C for 1 h (ramp rate of 10 °C min^{-1}) and cooled to 100 °C. The catalyst was then exposed to NH_3 gas (5% NH_3–95% He, 50 mL min^{-1}) at 100 °C, followed by evacuation at 100 °C for 3 h. Then, the desorbed NH_3 was measured from 100 °C to 700 °C with a heating rate of 5 °Cmin^{-1} in flow of He as a carrier gas at a flow rate of 40 mL min^{-1} until ammonia was desorbed completely.

Nature and strength of the acidity of the catalyst were determined by FTIR of adsorbed pyridine using Shimadzu 8000 series FT-IR using DRIFT assembly. The sample was placed in the DRIFT cell and heated to 400 °C in flow of inert gas (N_2) for 1 h. It was cooled to 100 °C and pyridine was adsorbed on the sample. The physisorbed pyridine was removed by flushing the cell with N_2 for 30 min at 100 °C. The temperature programmed desorption of pyridine was studied at 200, 300 and 400 °C. The spectra were recorded after maintaining the temperature for 30 min. The spectrum of the neat catalyst (before pyridine adsorption) at 100 °C was subtracted from all spectra.

2.3.7. Electron microscopic measurements

Scanning electron microscopic (SEM) measurements were performed on a FEI quanta 200 3D dual beam (ESEM) having thermionic emission tungsten filament in the 3 nm range at 30 kV. HRTEM analysis was done on a Tecnai G2-30 FEI instrument operating at an accelerating voltage of 300 kV. Before analysis, the powders were ultrasonically dispersed in *iso*-propanol, and two drops of *iso*-propanol containing the solid were deposited on a carbon coated copper grid.

2.4. Catalytic activity

2.4.1. Nitration of aromatics in batch mode

The nitration of aromatics was carried out in a 250 mL three necked round bottom flask fitted with Dean–Stark apparatus, reflux condenser and magnetic stirrer in an oil bath. The water formed during the nitration was removed azeotropically using ethylene

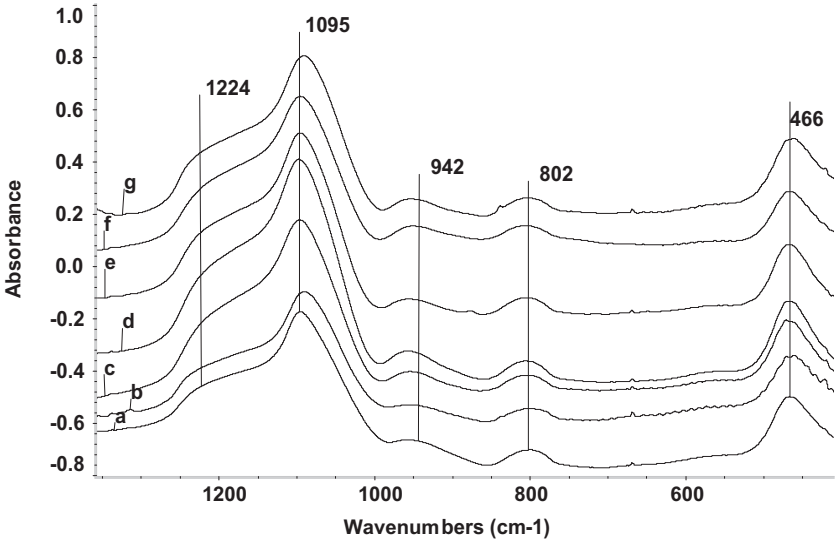

Fig. 3. FTIR spectra of (a) 1WSAMT, (b) 5WSAMT, (c) 10WSAMT, (d) 15WSAMT, (e) 20WSAMT, (f) 25WSAMT and (g) 30WSAMT.

dichloride (EDC) as solvent. Dean Stark apparatus meant for liquids with higher density than water was used in which the side arm is at bottom of the tube for flowing the solvent back to reaction mixture. Thus during azeotropic distillation high density ethylene dichloride (1.2 g/mL) remians at the bottom and water floats on the top. The EDC flows back from the bottom through the side arm to the reaction vessel and lower density water remains in the trap. The flask was charged with aromatic substrate, solvent (ethylene dichloride) and catalyst (20% by weight of substrate). Nitric acid was added dropwise to the reaction mixture. On completion of the reaction, the catalyst was filtered when hot and products were extracted with ethylene dichloride, washed sequentially with 5% aqueous solution of sodium bicarbonate, water and then dried with anhydrous Na_2SO_4. All the reactions were monitored by GC using GC-Hewlett Packard 6890 equipped with HP-5 column (50 m length, 0.25 mm internal diameter and 1 mm film thickness) and flame ionization detector (FID). Conversion of aromatics was calculated based upon the GC-FID results, where substrate conversion = [moles of substrate reacted]/[Initial moles of substrate used] × 100 and the selectivity of products was calculated by [total moles of the product formed]/[total moles of substrate converted] × 100. The individual yields were calculated and normalized with respect to the GC response factors. The product identification was carried out by injecting authentic samples in GC. In a few cases the products were isolated using column chromatography and characterised by ^{1}H NMR spectroscopy. The C-balance as well as the material balance was carried out for most of the experiments and they were found to be between 96 and 104%.

3. Results and discussion

A series of WS catalysts with WO_3 loading ranging from 1 to 30 wt% was prepared by sol gel method using ES-40 as silica precursor and ammonium metatungstate as WO_3 precursor. To study the effect of precursor on the catalyst structure 20WS was also prepared using tungstic acid and sodium tungstate as WO_3 precursors. As tungstic acid is not soluble in water it was converted to soluble tungsten peroxy species and further used for catalyst preparation.

3.1. Powder X-ray diffraction (PXRD) analysis

The PXRD patterns of the series of *x*WSAMT (*x* = 1, 5, 10, 15, 20, 25, 30 wt%) catalysts prepared using AMT as precursor are presented in Fig. 1. For comparison the XRD pattern of silica is also included in Fig. 1 (a). The pattern showed the amorphous nature of the material at 1% loading, indicating a very high dispersion of tungsten oxide on amorphous silica support. However, as the WO_3 loading was increased to 5 wt% and above upto 30 wt%, the XRD patterns exhibited sharp peaks corresponding to monoclinic WO_3 phase at 23.2, 23.6, 24.2, 26.6, 28.8 and 33.5° corresponding to (0 0 2), (0 2 0), (2 2 0) and (2 0 2) planes of monoclinic crystalline WO_3 phase (JCPDS no. 43-1035) on the broad underlying peak characteristic of the amorphous silica at $2\theta = 24°$.

The XRD patterns of 20WS catalysts synthesized using AMT, TA and NaT as precursors are shown in Fig. 2. Formation of crystalline WO_3 phase was observed in case of 20WSAMT (Fig. 2a) and 20WSTA (Fig. 2b) whereas 20WSNaT (Fig. 2c) showed dimerization of sodium tungstate to $Na_2W_2O_7$. The XRD peaks in 20WSNaT at 12.01, 16.05, 19.16, 27.5 and 28.9° corresponding to (0 0 2), (0 2 1), (1 1 2), (0 2 2), (2 0 2) and (2 2 0) planes respectively matched with peaks reported for $Na_2W_2O_7$ (JCPDS no. 70-0860). Due to dimerization of sodium tungstate no peaks for crystalline WO_3 species were observed. However in all the catalysts the presence of amorphous silica was observed at ~23.2°.

3.2. BET surface area analysis

The surface area of all the catalysts determined using BET method is given in Table 1. A high surface area of 606 m^2/g was observed in case of pure SiO_2 (PS) because of sol-gel technique using ES-40 as the silica source. The surface area of the catalysts decreased with increase in WO_3 loading. The surface area for WSAMT decreased from 505 to 368 m^2/g with increase in the WO_3 loading from 1 to 20 wt%. With further increase in WO_3 loading to 25 and 30 wt%, the surface area further decreased to 274 m^2/g. The pore volume for all the catalysts was in the range of 0.247–1.4 cc/g and pore size was in the range of 20–55 Å. Howevere there was no specific trend observed in pore size and pore volume of the catalysts. During the sol–gel synthesis, an aqueous solution of AMT was added to ES-40 which led to the simultaneous hydrolysis of ES-40. However, the rate of hydrolysis could not be maintained constant because the amount of water needed to dissolve AMT in each sample was not constant. The amount of water required for dissolving AMT was different in different WO_3 loading hence the rate of hydrolysis was not identical for each sample. Due to uncontrolled rate of hydrolysis there was no trend observed in sur-

Table 1
Surface area and acidity of the WO_3/SiO_2 series catalysts.

Sample	Surface area m^2/g	Pore volume cc/g	Pore radius Å	NH_3 desorbed mmol/g
SiO_2	606	0.93	42.5	0.03
1WSAMT	505	1.40	55.1	0.06
5WSAMT	393	0.36	20.4	0.14
10WSAMT	343	0.45	28.7	0.34
15WSAMT	332	0.99	44.5	0.35
20WSAMT	328	0.50	29.7	0.56
20 WSTA	217	0.37	34.2	0.22
20WSNaT	80	0.25	49.7	0.08
25WSAMT	275	0.54	39.6	0.52
30WSAMT	274	0.41	29.8	0.45

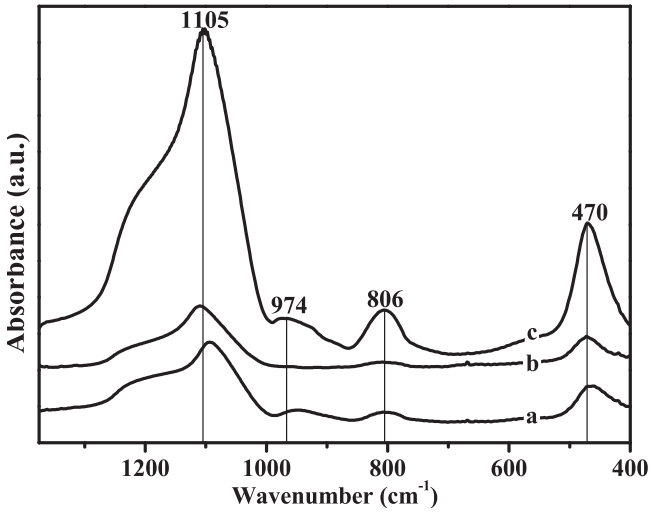

Fig. 4. FTIR spectra of (a) 20WSAMT (b) 20WSTA and (c) 20WSNaT.

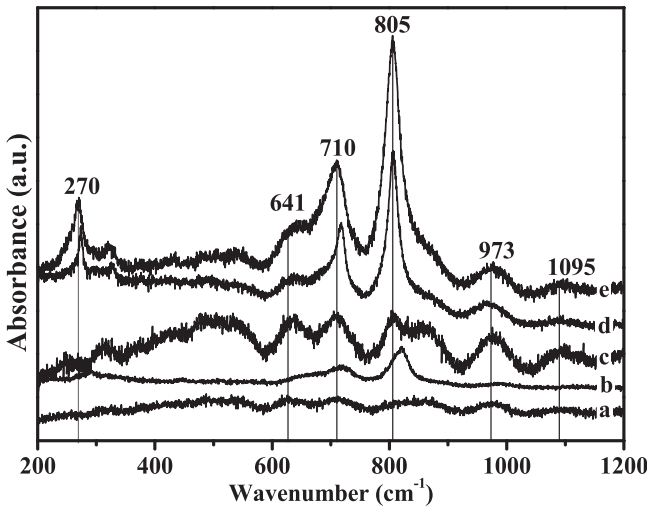

Fig. 5. Raman spectra of (a) 10WSAMT, (b) 15WSAMT, (c) 20WSAMT, (d) 25WSAMT and (e) 30WSAMT.

face area as well pore volume. As WO_3 loading was increased, the crystalline tungsten oxide clusters were formed that covered the amorphous silica support, reducing the total surface area of the catalyst. 20WSAMT showed 368 m^2/g surface area which decreased to 217 m^2/g when TA was used as precursor (20WSTA). There was substantial decrease in the surface area to only 80 m^2/g when NaT was used as precursor (20WSNaT). This drastic decrease in the surface area can be attributed to dimerisation of NaT on silica surface.

3.3. FTIR spectroscopic studies

KBr pelleted FTIR spectra of the series of WSAMT catalysts are presented in Fig. 3. The prominent bands around 1300–1000 cm^{-1} could be assigned to the asymmetric, symmetric stretching and bending vibrations of Si—O—Si, respectively whereas the bands at 942 and 802 cm^{-1} were due to the W=O_t and W—O—W stretching, respectively. The IR band at 468 cm^{-1} was due to O—Si—O bending vibrations.

When FTIR spectra of 20WS catalysts prepared by different precursor were compared (Fig. 4), 20WSNaT confirmed the formation of dimeric sodium tungstate which is in agreement with the XRD data. The spectrum of 20WSTA showed almost similar features as that of 20WSAMT.

3.4. Raman spectroscopic studies

Raman spectroscopy is an important tool for structural determination of oxide based catalysts. Raman spectra of the WSAMT catalysts are given in Fig. 5. Raman bands at 805, 710 and 270 cm^{-1} can be attributed to deformation and bending mode of W—O—W and W—O of crystalline WO_3. The band at 973 cm^{-1} can be assigned to isolated tetrahedral surface tungsten oxide O=W=O species. The band at 1095 cm^{-1} can be assigned to Si—O—Si stretch of the silica support.

3.5. UV–vis DRS analysis

To obtain information about the chemical nature and coordination states of tungsten oxide species, diffuse reflectance spectra in the UV–vis region of WO_3/SiO_2 samples were recorded (Fig. 6). This method is known to be highly sensitive for distinguishing species between incorporated metal and extra-framework metal oxides in different mesostructures [34,35]. For comparison UV–vis DRS spectra of bulk WO_3 and SiO_2 is also shown in Fig. 7. Three bands appeared at 206, 265, and 404 nm. The broad band at 206 nm can be attributed to tungsten trioxide [36,37]. The second broad band at about 265 nm corresponds to octahedral polytungstate species. Weber et al. showed that the low-energy absorption is shifted toward a lower wavelength with decreasing nuclearity of molybdenum or tungsten entities [38,39]. Therefore this broad band may be assigned to isolated tungsten oxide species or low nuclearity condensed oligomeric tungsten oxide species.

3.6. NH_3-TPD

NH_3-TPD experiments were carried out to determine the acid strength of the catalysts (Table 1). SiO_2 showed the lowest acidity with 0.03 mmol/g of ammonia desorbed at comparatively lower temperature (130 °C), indicating the presence of few weaker acid sites. Addition of 1% WO_3 to the silica support increased the acidity almost twice (0.06 mmol/g) with respect to the number of acid sites as well as the acid strength (NH_3 desorption at 144 °C). The tem-

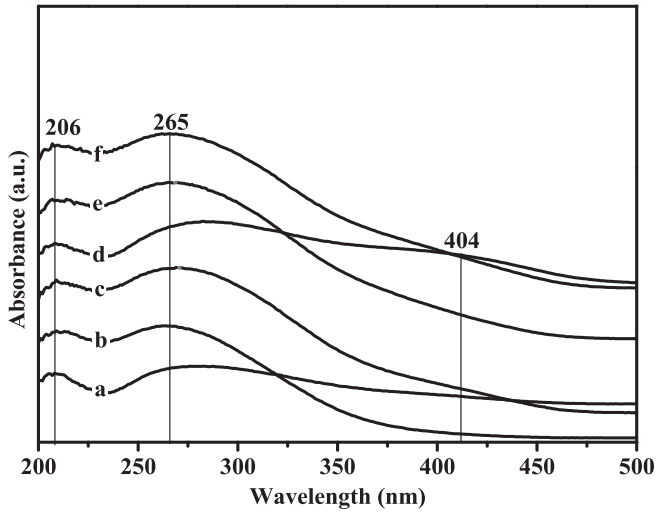

Fig. 6. UV–vis DRS analysis of (a)1WSAMT, (b) 10WSAMT, (c) 15WSAMT, (d) 20WSAMT, (e) 25WSAMT and f) 30WSAMT.

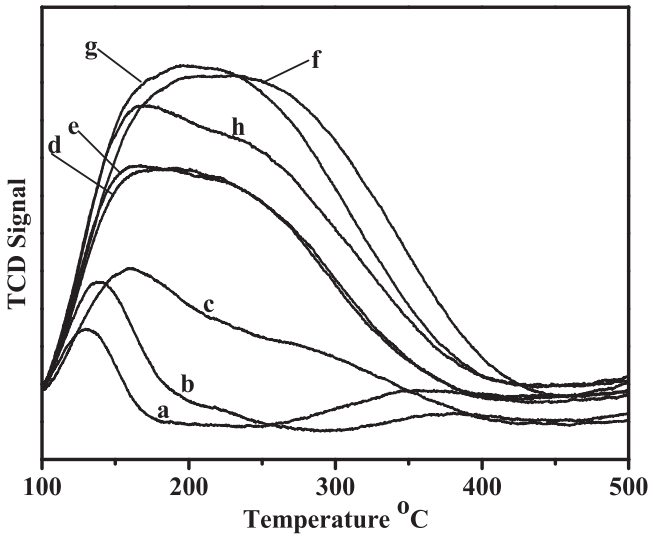

Fig. 8. NH_3-TPD of (a) SiO_2, (b) 1WSAMT, (c) 5WSAMT, (d) 10WSAMT, (e) 15WSAMT, (f) 20WSAMT, (g) 25WSAMT and (h) 30WSAMT.

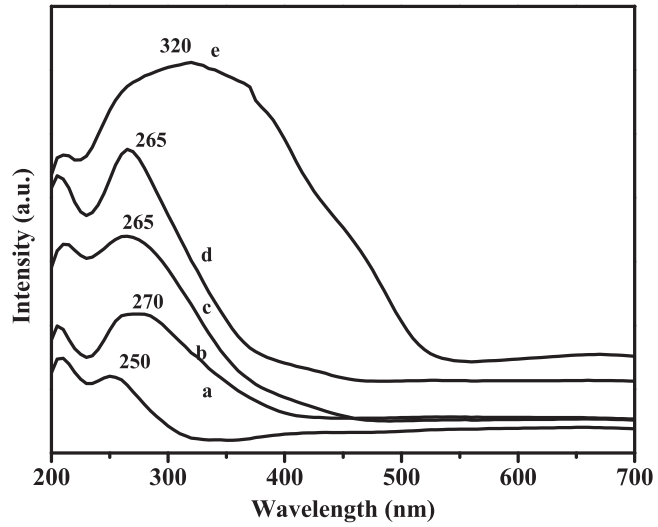

Fig. 7. UV–vis DRS analysis of (a) 20WSNaT, (b) SiO_2, (c) 20WSAMT, (d) 20WSTA and (e) WO_3.

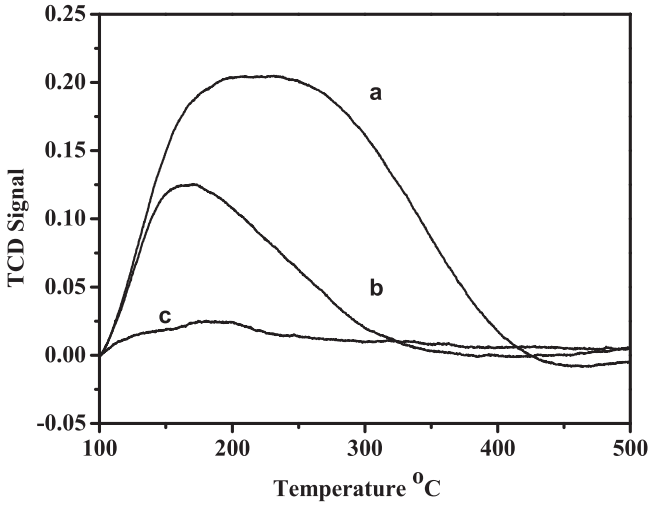

Fig. 9. NH_3-TPD of (a) 20WSAMT, (b) 20WSTA and (c) 20WSNaT.

perature for total desorption of ammonia increased (131–236 °C) with increase in WO_3 loading showing the increase in acid strength as well as in the number of acid sites. The catalyst with 20% WO_3 loading showed maximum number of acid sites (NH_3 desorbed: 0.56 mmol/g) as well as the highest acid strength. The ammonia desorption curve (Fig. 8f) indicated presence of maximum number of medium acid sites along with weak acid sites. The WO_3 loading above 20% did not show any further increase in the acidity, in fact acidity decreased upto 0.45 mmol/g with 30 wt% WO_3 loading. This may be attributed to agglomeration of WO_3 at higher loading. Thus 20 wt% WO_3 loading was found to be optimum loading to formation of maximum stronger acid sites within the series. 20WSTA and 20WSNaT showed total acidity of 0.22 and 0.08 mmol/g respectively (Fig. 9). The decreased acidity compared to 20WSAMT may be due to formation of dimeric ($Na_2W_2O_7$) species over silica. Thus 20WSAMT catalyst showed better acidity compared to 20WSTA and 20WSNaT catalysts.

3.7. FTIR of adsorbed pyridine

Nature of acidity on all the catalysts was evaluated by FTIR of adsorbed pyridine which revealed the presence of Lewis acidity in all WSAMT catalysts as shown in Fig. 10. Whereas, the presence of both Lewis and Brønsted acidity was observed at high WO_3 loadings. The spectra of 1WSAMT and 5WSAMT (Fig. 10 a, b) showed the presence of only Lewis acidity (peak at 1446 cm^{-1}) whereas above 5% WO_3 loading the catalysts showed presence of Brønsted acidity as well. With increase in the WO_3 loading from 1 to 20% there was gradual increase in Lewis as well as Brønsted acidity. However above 20% loading the acidity (Lewis and Brønsted) decreased which is in well agreement with NH_3-TPD analysis. As expected the Lewis acidity can be attributed to the presence of tungsten centre. However the generation of Brønsted acidity may be correlated to the formation of polytungstate species [40]. In present case also the formation of polytungstate was observed in UV–vis DRS analysis and hence the formation of Brønsted acidity could be attributed to the presence of polytungstate species. The observations were in good agreement with the findings from the UV–vis spectra of the samples (Fig. 6). The ratio of Brønsted to Lewis (B/L) acidity

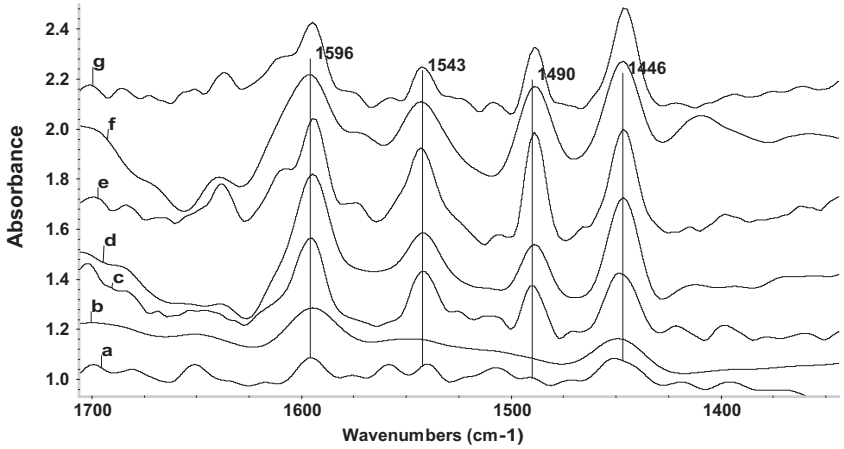

Fig. 10. FTIR spectra of adsorbed pyridine on (a) 1WSAMT, (b) 5WSAMT, (c) 10WSAMT, (d) 15WSAMT, (e) 20WSAMT, (f) 25WSAMT and (g) 30WSAMT at 100 °C after substraction of neat catalyst spectrum at 100 °C.

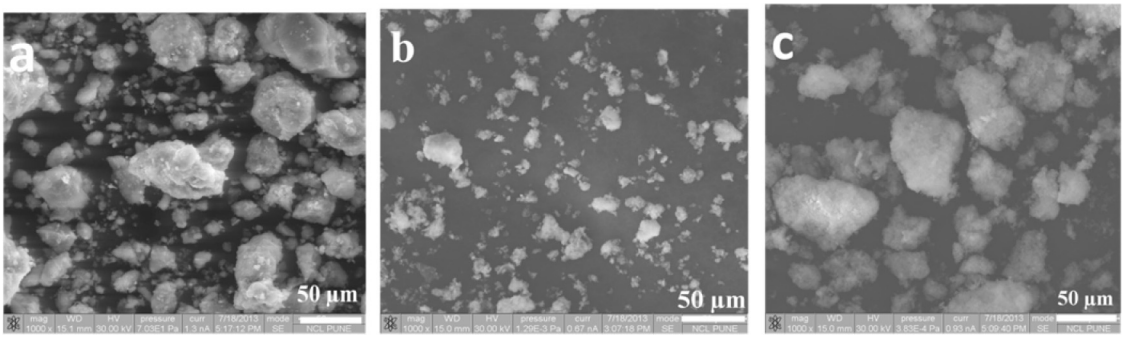

Fig. 11. SEM micrograph of (a) 20WSAMT, (b) 20WSTA and (c) 20WSNaT.

Table 2
Elemental analysis.

Samples	% Elemental composition				
	O K	Si K	W K	Na K	Total
20WSAMT	24.8	34.7	40.5	–	100
20WSTA	37.6	44.0	18.4	–	100
20WSNaT	36.6	43.4	18.4	1.6	100

increased with increase in WO_3 loading upto 20 wt% and decreased with further increase in WO_3 loading (Fig. 10).

3.8. SEM analysis

The EDAX analysis (Table 2) and morphology (Fig. 11) of 20WS prepared by different precursors showed the availability of more tungsten oxo species in case of 20WSAMT compared to 20WSTA and 20WSNaT. Presence of Na in 20WSNaT supports the XRD and FTIR analaysis for formation of dimeric sodium tungstate species on the surface. Due to sol gel preparation method some of the tungsten oxo species may get embedded in the bulk of the catalyst making it non available on the surface. This may be the reason for less availability of WOx species on surface in case of 20WSTA and 20WSNaT.

3.9. TEM analysis

TEM analysis (Fig. 12) of the 20WS catalysts showed formation of nano particles of tungsten oxide well dispersed on silica surface. The particle size was in the range of 2–5 nm in case of 20WSAMT (Fig. 12a). In the case of 20WSTA (Fig. 12b) the particle size was in the range of 2 to 8 nm, though the dispersion was not as uniform as 20WSAMT. Some agglomerated particles of WO_3 were also observed in 20WSTA. In case of 20WSNaT (Fig. 12c) slightly larger particles of 5–10 nm were observed dispersed on silica support.

In 20WSAMT the d- spacing observed was 3.86 Å and 3.64 Å (Fig. 13) corresponding to (0 0 2) and (2 0 0) planes of monoclinic phase of WO_3 respectively. The d spacing matched with the literature (JCPDS no. 43-1035) reconfirming presence of monoclinic WO_3.

3.10. Nitration of o-xylene

The prepared catalysts were evaluated for liquid phase nitration of range of aromatics (Scheme 1) using 70% nitric acid as nitrating agent and ethylene dichloride (EDC) as solvent to azeotropically remove the water formed in the reaction and the results are shown in Table 3. Initially nitration of *o*-xylene was carried out as *p*-nitrated product 4-nitro *o*-xylene (4-NOX) is commercially very important. The aim was to have maximum selectivity for 4-NOX and minimise oxidation products.

Blank reaction carried out without any catalyst for *o*-xylene nitration showed only 16% conversion with 62 and 26 % selectivity for 3-NOX and 4-NOX respectively along with the formation of 12% oxidation products (*o*-toluic acid and *o*-tolualdehyde). In absence of catalyst HNO_3 acts as very good oxidising agent. The high selectivity for oxidation products may be also attributed to absence of Brønsted acid in reaction mixture to protonate nitric acid to form nitronium ion for further nitration. NO_2 generated by decomposition of nitric acid under reaction conditions is very good oxidising agent. Hence in absence of Brønsted acidic catalyst, oxidation is predominant giving very high selectivity for oxidation

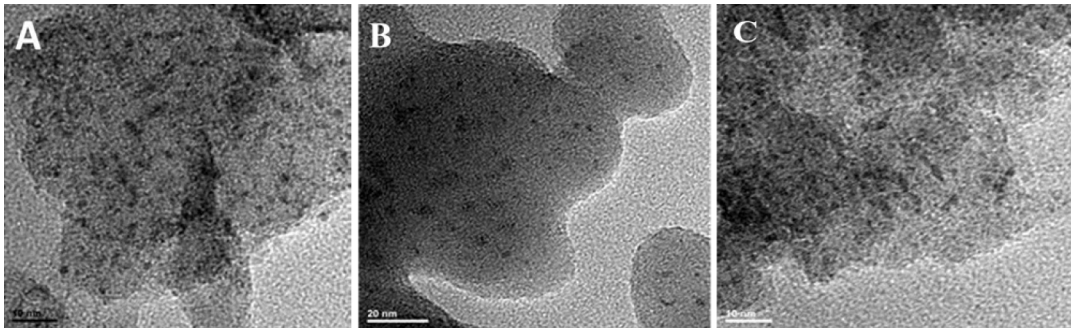

Fig. 12. TEM micrograph of (A) 20WSAMT, (B) 20WSNaT and (C) 20WSTA

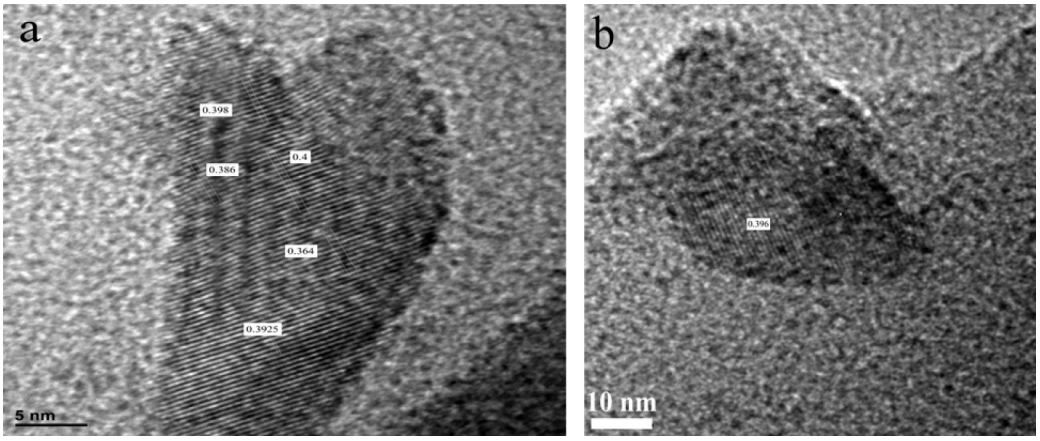

Fig. 13. TEM micrograph of 20WSAMT showing-spacing d- spacing.

Table 3
Effect of different loadings of WO_3 on SiO_2 for nitration of *o*-xylene.

Entry	WO_3 wt%	Conversion, %	Selectivity, %			4-NOX/3-NOX ratio
			3-NOX	4-NOX	OP	
1	Blank	16	62	26	12	0.4
2	WO_3	22	45	48	7	1.0
3	1WSAMT	55	49	51	00	1.0
4	5WSAMT	57	48	52	00	1.1
5	10WSAMT	61	48	51	1.0	1.0
6	15WSAMT	63	49	50	1.0	1.1
7	20WSAMT	68	45	54	1.0	1.2
8	20WSTA	63	49	50	1.0	1.0
9	20WSNaT	23	53	47	0	0.9
10	25WSAMT	61	48	52	0.0	1.1
11	30WSAMT	51	50	50	0.0	1.0

Reaction conditions: *o*-xylene: 70% HNO_3 1:1, catalyst 20 wt% of *o*-xylene, EDC (ethylene dichloride): 120 mL, temp. 90 °C, reaction time 8 h

products. The reaction carried out with only WO_3 for comparison showed marginally improved conversion (22%) with 45 and 48% selectivity for 3-NOX and 4-NOX respectively with formation of 7% oxidation products indicating weaker acid strength of only WO_3 for nitration to take place with 70% nitric acid as nitrating agent. The results also indicated that for getting better nitration activity the polytugngstate species needs to be well dispersed on the support which is achieved when silica is used as support by sol–gel process. Using 1WSAMT catalyst 32% *o*-xylene conversion was obtained with almost equal selectivity for 3-NOX and 4-NOX without the formation of any oxidation products. When WO_3 loading was gradually increased from 1% to 20%, there was a gradual increase in *o*-xylene conversion from 32 to 68%. However the selectivity ratio for 3-NOX/4-NOX was in the range of 49/51–45/55% with no formation of oxidation products. When WO_3 loading was further increased to 25 and 30% there was a decrease in the conversion though the selectivity was almost similar. With increase in WO_3 loading from 1 to 20% there was increase in total acidity as observed by NH_3-TPD measurements. FTIR of adsorbed pyridine revealed increase in Lewis as well as Brønsted acidity with increase in WO_3 loading upto 20%. As reported previously water gets polarised on tungsten based catalyst and transform Lewis acidity into Brønsted acidity. Also polytungstate species as observed by UV and Raman analysis are known to exhibit Brønsted acidity. This increased Lewis and Brønsted acidity with increase in the WO_3 loading from 1 to 20% has led to increase in nitration activity. At higher WO_3 loading agglomeration of WO_3 was observed which led to decrease in the acidity and in turn decrease in nitration activity.

When 20WS catalysts prepared using different precursors were compared, 20WSTA showed marginally lower conversion (63%) compared to 20WSAMT however, with 20WSNaT there was a significant decrease in the conversion to only 23% with higher selectivity for 3-NOX (53%). The results showed that AMT was the preferred precursor for the preparation of catalyst compared to TA and NaT. The catalyst prepared using sodium tungstate has shown almost no acidity by NH_3-TPD, hence very poor activity for nitration. In the literature it is well documented that replacement of H_2WO_4 by Na_2WO_4 decreases the activity due to change in the acidity of the catalyst [41]. In present case also sodium tugstate loaded silica catalyst has shown almost no acidity which has led to the poor nitration activity.

3.10.1. *Effect of HNO_3 concentration*

Various concentrations of HNO_3 ranging from 30 to 98% were used to study effect on *o*-xylene conversion and selectivity for 4-NOX and the results are given in Table 4. 30% HNO_3 gave only 27% conversion and equal selectivity for 3-NOX and 4-NOX. Whereas

Table 4
Effect of HNO_3 concentration on *o*-xylene nitration.

Entry	HNO_3 conc.%	Conv., %	Selectivity, %			4-NOX/3-NOX ratio
			3-NOX	4-NOX	OP	
1	30	27	49	49	2	1
2	70	68	45	54	1	1.2
3	90	75	49	50	1	1
4	98[a]	65[b]	67	4	29	0.1

Reaction conditions: *o*-xylene: HNO_3 1:1, catalyst 20WSAMT (20 wt% of reactant), EDC (ethylene dichloride): 120 mL, temp. 90 °C, reaction time 8 h.
[a] *o*-Xylene: HNO_3 5:1.
[b] Conversion w.r.t. HNO_3.

Table 5
Effect of molar ratios of reactants on *o*-xylene nitration.

Entry	*o*-Xylene:70% HNO_3 mole ratio	Conv., %	Selectivity, %			4-NOX/3-NOX ratio
			3-NOX	4-NOX	OP	
1	1:1	68	45	54	1	1.2
2	1:1.33	74	45	54	1	1.2
3	1:1.5	75	48	50	2	1.1
4	1:2	82	48	51	1	1.1

Reaction conditions: catalyst 20WSAMT (20 wt% of reactant), EDC (ethylene dichloride): 120 mL, temp. 90 °C, reaction time 8 h.

Table 6
Effect of catalyst loading w.r.t. substrate on *o*-xylene nitration.

Entry	% Catalyst loading w.r.t. substrate	Conv., %	Selectivity, %			4-NOX/3-NOX ratio
			3-NOX	4-NOX	OP	
1	10	65	44	55	1	1.2
2	20	68	45	54	1	1.2
3	30	70	45	54	1	1.2

Reaction conditions: catalyst 20WSAMT, *o*-xylene: 70% HNO_3 as 1:1, EDC (ethylene dichloride): 120 mL, temp. 90 °C, reaction time 8 h.

Table 7
Nitration of aromatics using 20WSAMT catalyst.

Entry	Substrate	Reaction time (h)	% Conversion	% Selectivity			
				2- Nitro	3- Nitro	4- Nitro	OP[a]
1	*o*-Xylene	8	74	–	45	54	1
2	Toluene	8	81	55	–	42	3.0
3	Phenol	6	100	46.5	–	46.5	7.0
4	*p*-Cresol	5.30	99	99	–	–	1.0
5	Chlorobenzene	8	55	38	–	62	0.0

Reaction conditions: substrate: 70% HNO_3 mole ratio 1:1.33, temp. 90 °C, EDC (ethylene dichloride) as solvent (50 mL).
[a] Oxidised products.

70% HNO_3 showed increased conversion up to 68% and slight increase in the selectivity for 4-NOX (54%). Increase in HNO_3 concentration to 90% further increased the *o*-xylene conversion to75% with 1:1 selectivity for 3-NOX and 4-NOX. But further increase in HNO_3 concentration to 98% decreased the conversion to 65% with increase in the formation of oxidation products (29%). Selectivity for 4-NOX also decreased to only 4% with 98% HNO_3. The significant decrease in the selectivity in case of 98% HNO_3 may be attributed to the highly exothermic nature of the reaction and subsequent decomposition of 98% HNO_3 at reaction temperature leading to formation of NO_2 which is very good oxidising agent. Due to the formation of NO_2 the selectivity for oxidised products increased considerably.

From the above data it is clear that 30% HNO_3 is very dilute for nitration to take place and 98% HNO_3 is too concentrated leading to highly exhothermic reaction with decomposition of nitric acid and formation of oxidation products. Hence 30 and 98% concentrations are not suitable nitrating agents for liquid phase nitration of aromatics. 70 and 90% HNO_3 showed comparable conversions (74%), though 70% HNO_3 gave slightly better selectivity for 4-NOX and it is easy to handle. Thus 70% HNO_3 was selected as nitrating agent for further optimisations.

3.10.2. o-Xylene: HNO_3 mole ratio

Effect of different molar ratios of nitric acid with respect to *o*-xylene on conversion and 4-NOX selectivity was studied and the results are given in Table 5. Stoichiometric (1:1) ratio of *o*-xylene: HNO_3 gave 68% conversion with 45/54 ratio of 3-/4-NOX. When the molar ratio was increased to 1:1.33 there was increase in the conversion to 74% with no change in the selectivity pattern. Further increasing the molar ratio to 1:2 led to further increase in the conversion to 82% with slight decrease in the selectivity for 4-NOX to 51%.

3.10.3. Effect of catalyst loading

Effect of different catalyst loading on *o*-xylene conversion and 4-NOX selectivity was studied by varyig the catalyst loading from 10 to 30 wt% with respect to substrate and the results are shown in Table 6. When catalyst loading was increased from 10 to 30% the *o*-xylene conversion increased from 65% to 70% without significantly affecting the selecivity for 4-NOX.

3.10.4. Nitration of various aromatic substrates

Various important aromatics were nitrated under optimized reaction conditions and the results are shown in Table 7. Toluene nitration (Table 7 entry 2) led to very high conversion of 81% with higher selectivity for o-nitro toluene (55%) with almost 4% selectivity for oxidised products. Phenol and *p*-cresol has shown almost complete conversion in only 6 h. In case of phenol the selectivity for *p*-nitro phenol was 46.5% with almost 7% selectivity for oxidation products (Table 7, entry 3). Whereas for *p*-cresol only 2-nitro *p*-cresol was obtained with 99% selectivity and 1% selectivity for oxidation products (Table 7, entry 4). When chlorobenzene was nitrated under identical conditions 55% conversion was obtained with 62% selectivity for *p*-nitrochlorobenzene and 38% selectivity for *o*-nitrochlorobenzene (Table 7, entry 5). From the nitration results in Table 7 it is clear that considerably higher conversion was obtained for aromatics with electron donating groups whereas lower conversion was obtained for aromatics with electron withdrawing substituents.

3.11. Proposed mechanism

Characterization of 20WSAMT revealed the presence of strong acidity with presence of both Lewis and Brønsted acid sites. For the nitration to occur generation of nitronium ion is essential and in turn Brønsted acidity is necessary. The FTIR of adsorbed pyridine revealed the presence of Brønsted acidity on 20WSAMT. The Brønsted acidity may be due to the presence of polytungstate species [40] or due to the polarisation of water molecule on 'W' centre. Based on the polarisation of water molecule on the catalyst the mechanism for nitronium ion generation and subsequent nitration of aromatics has been proposed (Scheme 2).

Due to the presence of metal centre the Lewis acidity is present on W of 20WSAMT. The water molecule can get polarised on W as shown in the scheme (A) generating Brønsted acidity. The acidic H^+ of polarised water can react with HNO_3 (B) generating nitronium ion (NO_2^+) and water as a by-product. The nitronium ion thus formed takes part in electrophilic substitution on aromatic ring (C) to give nitro product (D). In this study the formation of only mononitro product was observed without any dinitro product formation. Also the catalyst is not ordered mesoporous in nature hence the shape selective formation of one isomer was not observed.

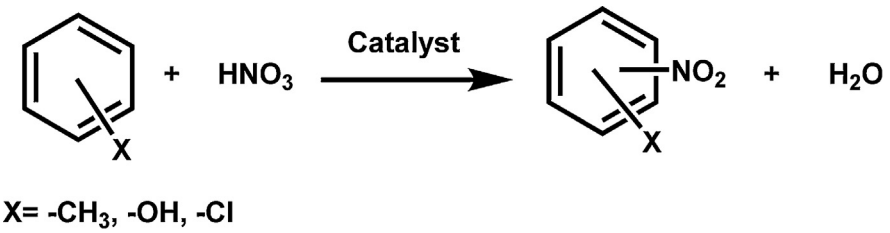

Scheme 1. General scheme for aromatic nitration.

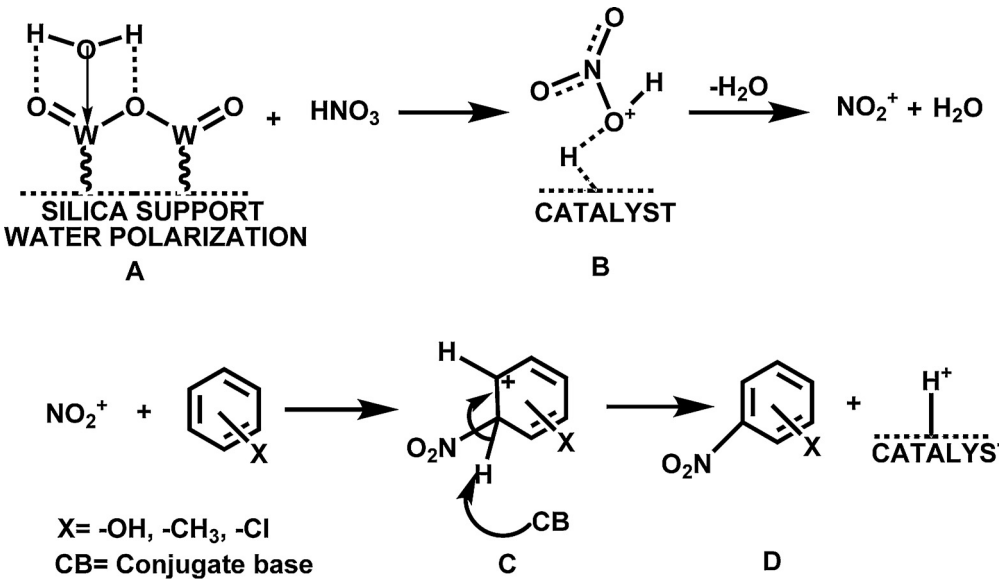

Scheme 2. Plausible nitration mechanism on WO_3/SiO_2 catalysts.

Though large number of solid acid catalysts like sulphated catalysts, modified clays, heterogenised heteropoly acids, zeolites and mixed metal oxides have been reported for liquid phase nitration of aromatics, the present catalytic system WO_3/SiO_2 has distinct advantages like (1) use of commercial 70% HNO_3 as nitrating agent (2) use of only slight excess of HNO_3 for nitration giving maximum yield (3) no use of hazardous solvent like acetic anhydride (4) high para selectivity (5) no high catalyst loading (6) minimum or no oxidation products (7) no side chain nitration products.

4. Conclusions

WO_3/SiO_2 prepared by sol gel method has shown formation of well dispersed WO_3 nano particles of 2–5 nm on high surface area mesoporous silica. The catalyst with 20 wt% WO_3 loading has shown the maximum acidity with presence of Lewis and Brønsted acid sites. The polarisation of water on tungsten centre led to the *in situ* formation of Brønsted acidity which in turn helps nitronium ion formation and subsequent nitration by electrophilic substitution reaction. The catalyst has shown very high efficiency for liquid phase nitration of aromatics using commercial 70% nitric acid as nitrating agent without using any sulfuric acid making this process an environmentally benign.

Acknowledgements

ABK acknowledges UGC for fellowship. Mr. A. Hardikar (FTIR), Mr. R. Gholap and Mr. K. Bhotkar (TEM, EDS) are acknowledged for their support in characterization. CSIR is acknowledged for research funding through XII FYP project CSC0125.

References

[1] N. Ono, The Nitro Group in Organic Synthesis, Wiley-VCH, New York, 2001.
[2] C.K. Ingold, Structure and Mechanism in Organic Chemistry, Second ed., Cornell Universiy Press, Ithaca, NY, 1969.
[3] G.A. Olah, S.J. Kuhn, in: G.A. Olah (Ed.), Friedel-Crafts and Related Reactions, 2, Wiley, New York, 1964.
[4] G.A. Olah, R. Malhotra, S.C. Narang, Nitration: Methods and Mechanism, in: H. Feuer (Ed.), VCH, New York, 1989.
[5] J.G. Hoggett, R.B. Moodie, J.R. Penton, K. Schofield, Nitration and Aromatic Reactivity, Cambridge University Press, London, 1971.
[6] K. Schofield, Aromatic Nitration, Cambridge University Press, London, 1980.
[7] L.V. Malysheva, E.A. Paukshits, K.G. Ione, Catal. Rev. Sci. Eng. 37 (1995) 179–226.
[8] G. Yan, M. Yang, Org. Biomol. Chem. 11 (2013) 2554–2566.
[9] C.Y. Chen, C.W. Wu, Y.S. Duh, Y.S.W. Yu, Process Saf. Environ. Prot. 76 (1998) 211–216.
[10] J.M. Riego, Z. Sedin, J.M. Zaldivar, N.C. Arziano, C. Tortato, Tet. Lett. 37 (1996) 513–516.
[11] W. Mao, H. Ma, B. Wang, J. Hazrd. Mater. 167 (2009) 707–712.
[12] D. Vassena, A. Kogelbauer, R. Prins, Catal. Today 60 (2000) 275–287.
[13] S.M. Mathew, A.V. Biradar, S.B. Umbarkar, M.K. Dongare, Catal. Commun. 7 (2006) 394–398.
[14] B.M. Choudary, M. Sateesh, M.L. Kantam, K.K. Rao, K.V.R. Prasad, K.V. Raghavan, J.A.R.P. Sarma, Chem. Commun. 1 (2000) 25–26.
[15] S.P. Dagade, V.S. Kadam, M.K. Dongare, Catal. Commun. 3 (2002) 67–70.
[16] P. Laszlo, J. Vandormeal, Chem. Lett. (1988) 1843–1846.
[17] B.M. Choudary, M.R. Sarma, K. Vijayakumar, J. Mol. Catal. 87 (1994) 33–38.
[18] K.R. Sunajadevi, S. Sugunan, Mater. Lett. 60 (2006) 3813–3817.
[19] A.S. Khder, A.I. Ahmed, Appl. Catal. A 354 (2009) 153–160.
[20] A. Hajipour, A.E. Ruoho, Tet. Lett. 46 (2005) 8307–8310.
[21] S. Gong, L. Liu, J. Zhang, Q. Cui, Process Saf. Environ. Prot. (2013) http://dx.doi.org/10.1016/j.psep.2013.03.005.
[22] K.M. Parida, D. Rath, J. Mol. Catal. A 258 (2006) 381–387.
[23] S. Mallick, K.M. Parida, Catal. Commun. 8 (2007) 1487–1492.
[24] P.T. Patil, K.M. Malshe, S.P. Dagade, M.K. Dongare, Catal. Commun. 4 (2003) 429–434.
[25] H. Sato, K. Hirose, Appl. Catal. A 174 (1998) 77–81.
[26] S.B. Umbarkar, A.V. Biradar, S.M. Mathew, S.B. Shelke, K.M. Malshe, P.T. Patil, S.P. Dagde, S.P. Niphadkar, M.K. Dongare, Green Chem. 8 (2006) 488–493.

[27] A. Shokrolahi, A. Zali, M.H. Keshavarz, Chin. Chem. Lett. 18 (2007) 1064–1066.
[28] X. Ma, B. Li, C. Lv, M. Lu, J. Wu, L. Liang, Catal. Lett. 141 (2011) 1814–1820.
[29] H. Pervez, S.O. Onyiriuka, L. Rees, C.J. Suckling, Tetrahedron 44 (1988) 4555–4568.
[30] S. Samajdar, F.F. Becker, B.K. Banik, Tet. Lett. 41 (2000) 8017–8020.
[31] V. Anuradha, P.V. Srinivas, P. Aparna, J.M. Rao, Tet. Lett. 47 (2006) 4933–4935.
[32] D. Koley, O.C. Colón, S.N. Savinov, Org. Lett. 11 (2009) 4172–4175.
[33] G.K.S. Prakash, C. Panja, T. Mathew, V. Surampudi, N.A. Petasis, G.A. Olah, Org. Lett. 6 (2004) 2205–2207.
[34] A. Stein, M. Fendorf, T.P. Jarvie, K.T. Mueller, A.J. Benesi, T.E. Mallouk, Chem. Mater. 7 (1995) 304–313.
[35] Y. Wand, O. Zhang, Y. Ohishi, T. Shishido, K. Takehira, Catal. Lett. 72 (2001) 215–219.
[36] E. Briot, J.Y. Piquemal, M. Vennat, J.M. Brégeault, G. Chottard, J.M. Manoli, J. Mater. Chem. 10 (2000) 953–958.
[37] O. Klepel, W. Böhlmann, E.B. Ivanov, V. Riede, H. Papp, Microporous Mesoporous Mater. 76 (2004) 105–112.
[38] R.S. Weber, J. Catal. 151 (1995) 470–474.
[39] E. Iglesia, D.G. Barton, S.L. Soled, S. Miseo, J.E. Baumgartner, W.E. Gates, G.A. Fuentes, G.D. Meitzner, Stud. Surf. Sci. Catal. 101 (1996) 533–542.
[40] A. Kido, H. Iwamoto, N. Azuma, A. Ueno, Catal. Surv. Asia 6 (2002) 45–53.
[41] P.T. Witte, Mechanisms in Homogeneous and Heterogeneous Epoxidation Catalysis, in: S.T. Oyama, F.W. Bull (Eds.), Elsevier, UK, 2008, Chapter 16.